Animal Nutriomics

cambridge.org/anr

Multi-omics evaluation of *Akkermansia muciniphila* intervention on LPS-challenged yellow-feathered broilers

Rongxia Zhu, Jie Tang, Yanrong Jing, Lijun Ou, Zecheng Zou, Caiyu Luo and Xin Feng

School of Animal Science and Technology, Foshan University, Foshan, China

Research Article

Cite this article: Zhu R, Tang J, Jing Y, Ou L, Zou Z, Luo C, Feng X (2026) Multi-omics evaluation of *Akkermansia muciniphila* intervention on LPS-challenged yellow-feathered broilers. *Animal Nutriomics* **3**, e1, 1–14. https://doi.org/10.1017/anr.2025.10019

Received: 5 May 2025
Revised: 1 September 2025
Accepted: 17 October 2025

Keywords:
Akkermansia muciniphila; lipopolysaccharide; broiler; 16S rDNA; transcriptome

Corresponding author: Xin Feng;
Email: 3haofx@gmail.com

Abstract

This study explored the effects of different preparations of *Akkermansia muciniphila* (AKK) on the gut microbiota and jejunal transcriptome of lipopolysaccharide (LPS) challenged yellow-feathered broilers. A total of 100 one-day-old broilers were divided into five groups, including control group (Control), LPS injection (LPS), gavage of AKK broth culture plus LPS injection (AKK), gavage of viable AKK suspension plus LPS injection (Active) and gavage of heat-inactivated AKK suspension plus LPS injection (Inactive). Growth performance results showed that LPS significantly reduced the body weight of broilers. Alpha diversity showed no significant group differences. At the phylum level, *Firmicutes* was significantly lower in groups with AKK gavage. At the genus level, *Bacteroides* was relatively more abundant, whereas *Streptococcus* was numerically less abundant in AKK-treated groups. The Active group had the highest abundance of *Akkermansia*. Transcriptome analysis revealed the Inactive group had significantly lower Occludin. Combined KEGG and GO analyses revealed that the LPS challenge suppressed innate immunity by downregulating the Retinoic acid-inducible gene (RIG)-I-like receptor signaling pathway. In response, different interventions distinctly modulated the transcriptome. The AKK group counteracted this suppression by upregulating innate immune and antiviral defense responses. The Active group primarily influenced metabolism, downregulating pathways for drug and glutathione metabolism and xenobiotic responses while upregulating retinol metabolism. In addition, the Inactive group demonstrated an upregulation of ribosome biogenesis, and energy metabolism, suggesting a restoration of core cellular functions. In summary, all gavaged AKK preparations maintained broiler gut microbiome stability, while AKK broth culture demonstrated superior efficacy in alleviating LPS-induced jejunal stress.

Introduction

The physiological state of livestock and poultry is affected by a variety of factors, such as high temperature, low sanitary conditions, disease stimulation, etc. These factors are prone to trigger the oxidative stress response of the organism, which has an impact on the health status and production performance of livestock and poultry (Mishra and Jha 2019). Gut health and function play a key role in poultry production. The gut microbiota consists mainly of bacteria, fungi and protozoa (Gabriel et al. 2006). When oxidative stress occurs in poultry, it triggers an inflammatory response that disrupts the intestinal barrier and micro-ecological balance (Elokil et al. 2024; Kikusato and Toyomizu 2023).

Akkermansia muciniphila (AKK) is an oval-shaped gram-negative bacterium that is recognized as a "next-generation probiotic" (Chelakkot et al. 2018; Zhang et al. 2019). AKK primarily uses human intestinal mucus as its source of carbon and nitrogen (Aggarwal et al. 2022). Some studies have shown that AKK regulates the intestinal barrier by modulating the tight junction (TJ) proteins Claudin-3 and Occludin (Chelakkot et al. 2018; Plovier et al. 2017). Ottman et al. (2017) found that AKK treatment increased the transepithelial cellular resistance of human clonal colon cancer cells (Caco-2 cells) in *in vitro* studies, as evidenced by enhanced intestinal epithelial barrier function (Ottman et al. 2017). Studies have shown that AKK is associated with human health, and its metabolite propionic acid, which demonstrates immunomodulatory effects in the body (Lukovac et al. 2014). A study by Plovier et al. (2017) found that AKK, even after pasteurization and inactivation, retained the ability to reduce insulin resistance and improve dyslipidemia. Furthermore, research demonstrates that AKK alleviates lipopolysaccharide (LPS)-induced intestinal dysfunction through restoration of gut microbiota homeostasis and modulation of immune responses (Hu et al. 2025).

© The Author(s), 2026. Published by Cambridge University Press on behalf of Zhejiang University and Zhejiang University Press. This is an Open Access article, distributed under the terms of the Creative Commons Attribution licence (http://creativecommons.org/licenses/by/4.0), which permits unrestricted re-use, distribution and reproduction, provided the original article is properly cited.

Current research on AKK has primarily focused on humans and murine models, with limited exploration of its effects in livestock and poultry. In this study, we utilized LPS to establish a stress model in broilers, investigating how different preparations of AKK (AKK broth culture, viable AKK suspension and inactivated AKK suspension) modulate gut microbiome composition and jejunum health post-stress. This work aims to provide a scientific foundation for leveraging AKK in poultry production and stress mitigation strategies.

Materials and methods

Preparation of AKK

AKK (ATCC BAA-835) was anaerobically cultured in mucin-containing broth medium (1% porcine gastric mucin, 0.5% tryptone, 0.2% yeast extract, pH 6.8) at 37°C for 72 hours and harvested at late-log phase (OD600 ≈ 0.8–1.0). For the preparation of a viable AKK suspension, the AKK broth culture was centrifuged at 8,000× g for 10 min at 4°C to pellet bacterial cells. The supernatant was discarded, and the bacterial pellet was washed twice with sterile phosphate-buffered saline (PBS, pH 7.4). Finally, the cells were resuspended in PBS to a final concentration of 1×10^8 colony-forming units (CFU)/mL. For the heat-inactivated AKK suspension, the AKK pellet was resuspended in PBS and subjected to heat inactivation at 80°C for 30 min. The viability and inactivation of AKK cells were verified by culturing the treated suspension on agar plates.

Animal experimental design

One hundred one-day-old healthy male Lingnan yellow-feathered broilers were randomly divided into five groups. Each group had four replicates with five chickens per replicate. Control group (gavage of 1 mL PBS and intraperitoneal injection of an equal amount of saline); LPS group (gavage of 1 mL PBS and intraperitoneal injection of 0.5 mg/kg BW LPS); AKK group (gavage of 1 mL 10^8 CFU/mL AKK with culture medium and intraperitoneal injection of 0.5 mg/kg BW LPS); Active group (gavage of 1 mL 10^8 CFU/mL viable AKK suspension and intraperitoneal injection of 0.5 mg/kg BW LPS); Inactive group (gavage of 1 mL 10^8 CFU/mL heat-inactivated AKK suspension and intraperitoneal injection of 0.5 mg/kg BW LPS). Oral gavage with different AKK preparations was administered on days 7, 9, 11, 13, 15 and 17, while intraperitoneal injections were performed on days 17, 19 and 21. LPS from *Escherichia coli* O55:B5 (Product No. L2880, Sigma-Aldrich, St. Louis, MO, USA) was used to induce the stress model. Throughout the study, broiler chicks were housed under controlled environmental conditions with *ad libitum* access to water and a corn-soybean meal-based basal diet (Table 1). The coop temperature was maintained at 32°C–33°C during the first week, and gradually decreased to 24°C by the end of the third week. Throughout the experimental period, all birds remained clinically healthy, and no mortality was recorded. Feed intake and body weight were monitored to evaluate growth performance, including average daily gain (ADG), average daily feed intake (ADFI) and feed conversion ratio. On day 22, following a 12-hour fasting period, one bird per replicate ($n = 4$) was randomly selected and humanely euthanized by cervical dislocation. Cecal digesta and jejunal mucosa samples were collected for downstream analysis.

Table 1. The ingredients and nutrient composition of the basal diet

Ingredient composition, %	
Corn	44.5
Soybean meal (CP = 46%)	33.5
Extruded soybeans	5
Sorghum	10
Lard	1.5
Fish meal	1.3
Dicalcium phosphate	1.3
Limestone	1.4
L-lysine hydrochloride	0.25
DL-methionine	0.23
L-threonine	0.05
Premix compound	0.71
Sodium chloride	0.12
Choline chloride	0.12
Antioxidant	0.01
Phytase	0.01
Calculated nutrient composition	
Crude protein	21.45
Metabolizable energy (kcal/kg)	2,877
Crude fat	4.87
Calcium	1.00
Total phosphorus	0.64
Available phosphorus	0.49
Lysine	1.39
Methionine	0.56
Threonine	0.88

Note: (1) Premix provided per kilogram of the diet: vitamin A 12,000 IU; vitamin D_3 3000 IU; vitamin E 10 IU; vitamin K_3 2 mg; vitamin B_1 1 mg; vitamin B_2 3 mg; vitamin B_6 2 mg; vitamin B_{12} 0.01 mg; niacin 20 mg; pantothenic acid 4 mg; folic acid 0.54 mg; biotin 0.05 mg; Fe 100 mg; Cu 20 mg; Mn 100 mg; Zn 80 mg; I 3 mg; Se 0.5 mg. (2) Antioxidant: The antioxidants used in the premix are Butylated Hydroxytoluene (BHT) and Tert-butylhydroquinone (TBHQ).

16S rDNA analysis of the gut microbiota

Genomic DNA was extracted from the contents of the cecum using the cetyltrimethylammonium bromide method (Trojánek et al. 2018). Then the purity and concentration of DNA were detected by 1% agarose gel electrophoresis. The appropriate amount of sample DNA was put into a centrifuge tube and diluted to 1 ng/μL with sterile water. After DNA extraction, the V3–V4 region of the 16S rRNA gene was amplified with primers 341 F (5'-CCTAYGGGRBGCASCAG-3') and 806 R (5'-GGACTACNNGGGGTATCTAAT-3'). The PCR products were mixed in equal amounts according to the concentration, and the PCR products were detected by agarose gel electrophoresis with 2% agarose after sufficient mixing. The products were recovered using the Universal DNA Purification and Recovery Kit (TianGen) for the target bands. The library was constructed, and the constructed library was quantified by Qubit and Q-PCR. After the library was qualified, NovaSeq6000 was used to perform PE250

https://doi.org/10.1017/anr.2025.10019 Published online by Cambridge University Press

Table 2. Effect of *Akkermansia muciniphila* on the growth performance of lipopolysaccharide-challenged yellow-feathered broilers

Items	Control	LPS	AKK	Active	Inactive	SEM	*P*
Initial weight, g	33.41	32.89	33.13	33.06	33.41	0.120	0.63
Final weight, g	500.60[a]	475.90[c]	492.87[ab]	471.65[c]	482.87[bc]	3.052	0.002
Average daily gain, g	22.25[a]	21.10[c]	21.89[ab]	20.88[c]	21.40[bc]	0.214	0.002
Average daily feed intake, g	32.26	31.12	32.59	31.25	32.79	0.456	0.73
Feed conversion ratio	1.45	1.48	1.49	1.50	1.53	0.020	0.82

Note: Control: gavage with phosphate-buffered saline (PBS) and intraperitoneal injection of saline; LPS: gavage with PBS and administered intraperitoneally with lipopolysaccharide (LPS); AKK: gavage with *Akkermansia muciniphila* in culture medium and administered intraperitoneally with LPS; Active: gavage with live *Akkermansia muciniphila* resuspended in PBS and administered intraperitoneally with LPS; Inactive: gavage with inactivated *Akkermansia muciniphila* resuspended in PBS and administered intraperitoneally with LPS; SEM: standard error of mean; [a,b,c] Means in the same row with different superscript letters differ significantly ($P < 0.05$).

on-line sequencing to obtain the raw data. Then the raw data were spliced and filtered to obtain clean data. Based on the valid data, DADA2 was used for noise reduction to obtain the final ASVs (Li et al. 2020).

The obtained ASVs were subjected to species annotation, Alpha diversity analysis and Beta diversity analysis using QIIME2 software. A Venn diagram of ASVs was created using R (Version 3.5.3; Venn Diagram package). Principal coordinates analysis (PCoA) analyses were calculated and plotted by the ade4 package and ggplot2 package in R software (version 4.0.3). Linear discriminant analysis (LEfSe) effect size was performed using LEfSe software with a default linear discriminant analysis (LDA) score threshold of 2.0 (Segata et al. 2011). Finally, the microbial community was analyzed for functional prediction using PICRUSt 2 software (Douglas et al. 2020).

RNA extraction and transcriptome sequencing

Total RNA was extracted from the jejunal mucosa with TRIzol reagent (Invitrogen, Carlsbad, CA, USA) according to the manufacturer's instructions, and then accurately examined for RNA integrity using an Agilent 2100 bioanalyzer. The mRNAs with polyA tails were enriched by Oligo magnetic beads, and then the obtained mRNAs were randomly interrupted with divalent cations in NEB Fragmentation Buffer, and the libraries were constructed according to the NEB common library construction method (Parkhomchuk et al. 2009). The different libraries were subjected to Illumina sequencing to obtain raw data. The raw data were then filtered to obtain clean data, and the paired-end clean reads were compared to the reference genome using HISAT2 v2.0.5. The FPKM for each gene was then calculated based on the length of the gene, and the number of reads mapped to that gene was calculated using featureCounts (1.5.0-p3). Differential expression analysis between the two comparison combinations was performed using DESeq2 software (1.20.0), and the resulting *P*-values were adjusted to control for false discovery rates using the method of Benjamini and Hochberg. Genes with $|\log2(\text{FoldChange})| \geq 1$ and adjusted *P*-values ≤ 0.05 were assigned as differentially expressed. KEGG analysis and GO enrichment analysis of differentially expressed genes (DEGs) were achieved by clusterProfiler (3.8.1) software.

Statistical analysis

The experimental data were analyzed by one-way analysis of variance (SPSS 27.0). The following statistical model was used: $Y_{ijk} = \mu + T_i + \varepsilon_{ij}$, where Y_{ijk} = measured response, μ = overall mean, T_i = fixed effect of treatment ($i = 1$ to 5) and ε_{ij} = residuals. Duncan's method was employed for multiple comparisons upon significance. Significance was declared at $P \leq 0.05$.

Results

Determination of growth performance

LPS significantly decreased the final weight and ADG of broilers ($P < 0.05$; Table 2). There was no significant difference in ADFI among the five groups. Notably, the addition of AKK broth culture completely counteracted the LPS-induced growth depression. There were no significant differences in final body weight and ADG between the AKK group and the Control group.

Similarity analysis and alpha diversity analysis

After data filtering, quality control and chimeric sequence removal, valid data were obtained (Table 3). The number of valid data bases of all samples ranged from 23, 634, 939 to 41, 431, 813 nt, and the average length ranged from 409.76 to 417.18 nt. While the GC, Q20 and Q30 were above 50%, 98% and 90%, respectively.

A total of 1,403 amplicon sequence variants (ASVs) were identified from 20 samples (Fig. 1). Among these, 278 ASVs were shared by all groups, while unique ASV counts were observed in the Control (151), LPS (199), AKK (165), Active (190) and Inactive (149) groups, respectively. There was no significant difference in chao1, dominance, goods_coverage, observed_features, pielou_e, shannon and simpson indices among the five groups (Table 4).

The results of PCoA analysis revealed that the first and second principal components accounted for 28.73% and 13.52% of the total variance, respectively (Fig. 2). No significant separation was observed between samples from different groups. Anosim similarity analysis indicated that the between-group difference for Control-LPS was significantly greater than the within-group difference (*R*-value > 0, *P*-value < 0.05). For other group comparisons (excluding AKK-inactive group), while the between-group differences were nominally greater than within-group differences, these results did not reach statistical significance (*R*-value > 0, *P*-value > 0.05).

Analysis of gut microbial composition

Firmicutes, Bacteroidota and *Verrucomicrobiota* were the dominant phyla (Table 5) while *Firmicutes* in the Control group was significantly more abundant than the AKK, Active and Inactive groups ($P < 0.05$). At the genus level, *Bacteroides, Alistipes* and *Akkermansia* were identified as dominant genera. The abundance of *Alistipes* in the Active group was significantly lower than in

https://doi.org/10.1017/anr.2025.10019 Published online by Cambridge University Press

Table 3. Statistical information of obtained effective tags during data processing for 16S rDNA sequencing

Sample	Base (nt)	Avglen (nt)	GC (%)	Q20 (%)	Q30 (%)
Control1	37,831,041	410.97	51.92	98.53	95.06
Control2	37,427,527	409.76	52.43	98.65	95.33
Control3	35,212,089	411.18	51.93	98.70	95.42
Control4	32,538,427	412.65	52.04	98.45	94.79
LPS1	34,840,159	410.27	52.09	98.57	95.09
LPS2	33,671,780	413.04	51.65	98.43	94.62
LPS3	35,461,541	415.95	51.28	98.35	94.48
LPS4	35,184,034	412.09	51.92	98.50	94.86
AKK1	35,680,100	412.81	51.32	98.50	94.92
AKK2	37,533,995	414.47	50.85	98.40	94.70
AKK3	34,937,046	412.35	51.91	98.44	94.79
AKK4	35,985,241	414.49	51.15	98.36	94.52
Active1	40,373,403	415.45	49.79	98.56	95.01
Active2	37,061,236	414.14	51.30	98.69	95.39
Active3	30,812,725	411.92	52.18	98.51	94.85
Active4	38,855,804	415.42	50.03	98.53	94.94
Inactive1	41,431,813	417.18	49.72	98.55	95.04
Inactive2	39,833,116	412.58	51.69	98.52	95.00
Inactive3	23,634,939	410.79	52.36	98.61	95.17
Inactive4	35,019,697	411.42	51.64	98.60	95.12

Note: Base (nt): is the number of effective tags; Avglen (nt): refers to the average length of effective tags; Q20 (%) and Q30 (%): refer to the percentage of total effective tags for bases with mass values greater than or equal to 20 and 30, respectively; GC (%): indicates the content of GC bases in effective tags.

the AKK and Inactive groups ($P < 0.05$). Similarly, *Streptococcus* was also comparatively lower in the AKK group, Active group and Inactive groups. In contrast, *Akkermansia* and *Bacteroides* exhibited higher relative abundances in the AKK-gavaged group, with *Akkermansia* reaching its peak abundance in the Active group (Table 6).

Enriched biomarker taxa were identified at the genus level using LefSe analysis (LDA > 2.0). A total of seven biomarker-bacterial genera were identified in the Control, LPS, AKK and Inactive groups. Among them, *Lachnospiraceae_NC2004_group* was enriched in LPS group, *GCA_900066575* was enriched in Inactive group, *Ruminococcus, NK4A214_group, UCS_1_2E3* and *Merdibacter* were enriched in Control group, *Alistipes* was enriched in the AKK group (Fig. 3).

RNA sequence data summary and correlation analysis

A total of 927,366,014 raw reads were obtained from 20 samples. More than 98% of the bases had quality values greater than 20, and more than 97% of the bases had quality values greater than 30 (Table 7). The sequencing data can meet the standard of subsequent sequencing. Correlation analysis was performed between the samples, and the R^2 between each group of samples was more than 0.8 (Fig. 4A). Principal component analysis of gene expression values across all samples revealed limited group separation, with the first two principal components (PC1: 27.04%, PC2: 11.35%) collectively explaining 38.39% of the total variance (Fig. 4B). The ordination plot showed no distinct clustering among the five experimental groups.

Differential expression analysis

In this study, DEGs were identified using thresholds of $|\log2(\text{FoldChange})| \geq 1$ and adjusted P-value ≤ 0.05 (Fig. 5). Differential gene expression analysis revealed distinct patterns across group comparisons. The LPS vs Control group exhibited 259 DEGs (116 upregulated, 143 downregulated), while the AKK vs LPS comparison showed 369 DEGs (252 upregulated, 117 downregulated). The Active vs LPS group had 256 DEGs (112 upregulated, 144 downregulated), whereas the Inactive vs LPS group displayed the highest number of DEGs (1,100; 558 upregulated, 542 downregulated).

The expression of the Occludin gene in the Inactive group was significantly lower than that in the other four groups ($P < 0.05$). While no significant differences were detected in Claudin-1, Claudin-2, or Claudin-3 expression across groups, the Inactive group exhibited consistently lower expression levels of these TJ proteins compared to the other four groups (Table 8).

KEGG pathway enrichment analysis

KEGG pathway enrichment analysis was performed on the DEGs for each pairwise comparison. The top ten significantly enriched pathways ($P < 0.05$) from the LPS vs Control, AKK vs LPS, Active vs LPS and Inactive vs LPS comparisons were identified and are summarized in Table 9. The RIG-I-like receptor signaling pathway was downregulated in the LPS vs Control comparison. The NOD-like receptor signaling pathway and RIG-I-like receptor signaling pathway exhibited significant enrichment ($P < 0.05$) in the AKK vs LPS comparison. Nine pathways were significantly enriched in the Active vs LPS comparison, all of which were downregulated except retinol metabolism. In the Inactive vs LPS comparison, all pathways exhibited downregulation except ribosome, oxidative phosphorylation and cardiac muscle contraction pathways.

Gene Ontology function enrichment analysis

Gene Ontology (GO) enrichment analysis categorized results into three ontological domains: biological process (BP), cellular composition and molecular function. The top ten significantly enriched terms from each domain were selected for visualization, with results displayed in Fig. 6. GO enrichment analysis across the four comparisons revealed significant enrichment in terms related to exogenous substance metabolism, energy metabolism, viral defense responses, cellular structure, signal regulation and enzyme activity. In the LPS vs Control comparison, GO enrichment analysis indicated a broad upregulation across most BPs. In contrast, only three terms showed significant downregulation, including actomyosin structure organization, regulation of lipid metabolic process and positive regulation of catabolic process. GO enrichment analysis of the AKK vs LPS comparison indicated a broad functional upregulation, suggesting a strong restorative effect. The significantly upregulated terms were primarily clustered into key biological functions, including viral defense responses (defense response to virus), metabolic processes (phosphate-containing compound metabolic process, phosphorus metabolic process), regulation of cell communication and nucleotide binding activities (guanyl nucleotide binding, guanyl ribonucleotide binding, GTP

https://doi.org/10.1017/anr.2025.10019 Published online by Cambridge University Press

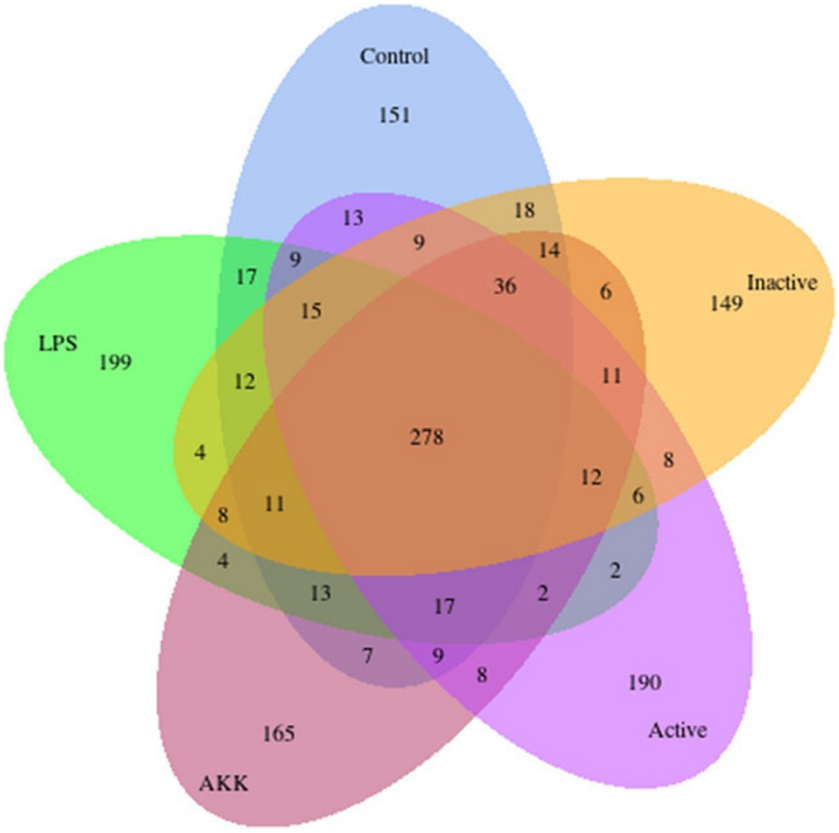


Figure 1. Venn diagram of shared ASVs in five groups.

Table 4. Effect of *Akkermansia muciniphila* on alpha diversity indices of gut microbiota in lipopolysaccharide-challenged yellow-feathered broiler chickens

Items	Control	LPS	AKK	Active	Inactive	SEM	*P*
Chao1	365.74	310.50	315.32	332.44	314.94	9.488	0.35
Dominance	0.05	0.10	0.11	0.10	0.10	0.008	0.25
Goods_coverage	1.00	1.00	1.00	0.9998	1.00	0.000 05	0.44
Observed_features	361.00	306.25	312.25	322.25	311.75	9.386	0.37
Pielou_e	0.70	0.63	0.63	0.60	0.63	0.012	0.10
Shannon	5.97	5.18	5.19	5.03	5.22	0.124	0.11
Simpson	0.95	0.90	0.89	0.90	0.90	0.008	0.25

Note: Control: gavage with phosphate-buffered saline (PBS) and intraperitoneal injection of saline; LPS: gavage with PBS and administered intraperitoneally with lipopolysaccharide (LPS); AKK: gavage with *Akkermansia muciniphila* in culture medium and administered intraperitoneally with LPS; Active: gavage with live *Akkermansia muciniphila* resuspended in PBS and administered intraperitoneally with LPS; Inactive: gavage with inactivated *Akkermansia muciniphila* resuspended in PBS and administered intraperitoneally with LPS; SEM: standard error of mean.

binding), along with growth factor receptor binding. Compared to the LPS group, the Active group exhibited a transcriptomic signature indicative of reduced cellular stress. This was primarily characterized by a significant downregulation of pathways involved in detoxifying foreign compounds (xenobiotic metabolic process) and a broad suppression of oxidoreductase activities. Compared to the LPS group, the Inactive group exhibited a significant upregulation in the entire protein synthesis machinery, including terms related to ribosomes. Concurrently, pathways for energy production were strongly reactivated (oxidative phosphorylation; respiratory electron transport chain). This was complemented by an enhanced metabolism of nucleotides and energy carriers like ATP. Furthermore, a specific class of oxidoreductase activity, acting on NAD(P)H, was also upregulated, indicating a restoration of cellular metabolic and redox homeostasis.

Discussion

AKK, considered as a next-generation probiotic, is thought to strengthen the gut barrier and reduce inflammatory responses (Shen et al. 2016). Oral administration of AKK increased jejunal core bacterial abundance and inhibited lipid absorption in the proximal jejunum (Ma et al. 2025). AKK enhances intestinal barrier integrity through the production of short-chain fatty acids (SCFAs) (Zhang and Wang 2023). Previous studies have shown that LPS has a negative effect on broiler growth performance (Song et al. 2025; Zhang et al. 2023). In the present study, the final weight and ADG of the animals were significantly lower than those of the Control group, confirming the successful induction of stress model through LPS challenge. The protective effect on growth appeared to be unique to the AKK broth culture. While the AKK

https://doi.org/10.1017/anr.2025.10019 Published online by Cambridge University Press

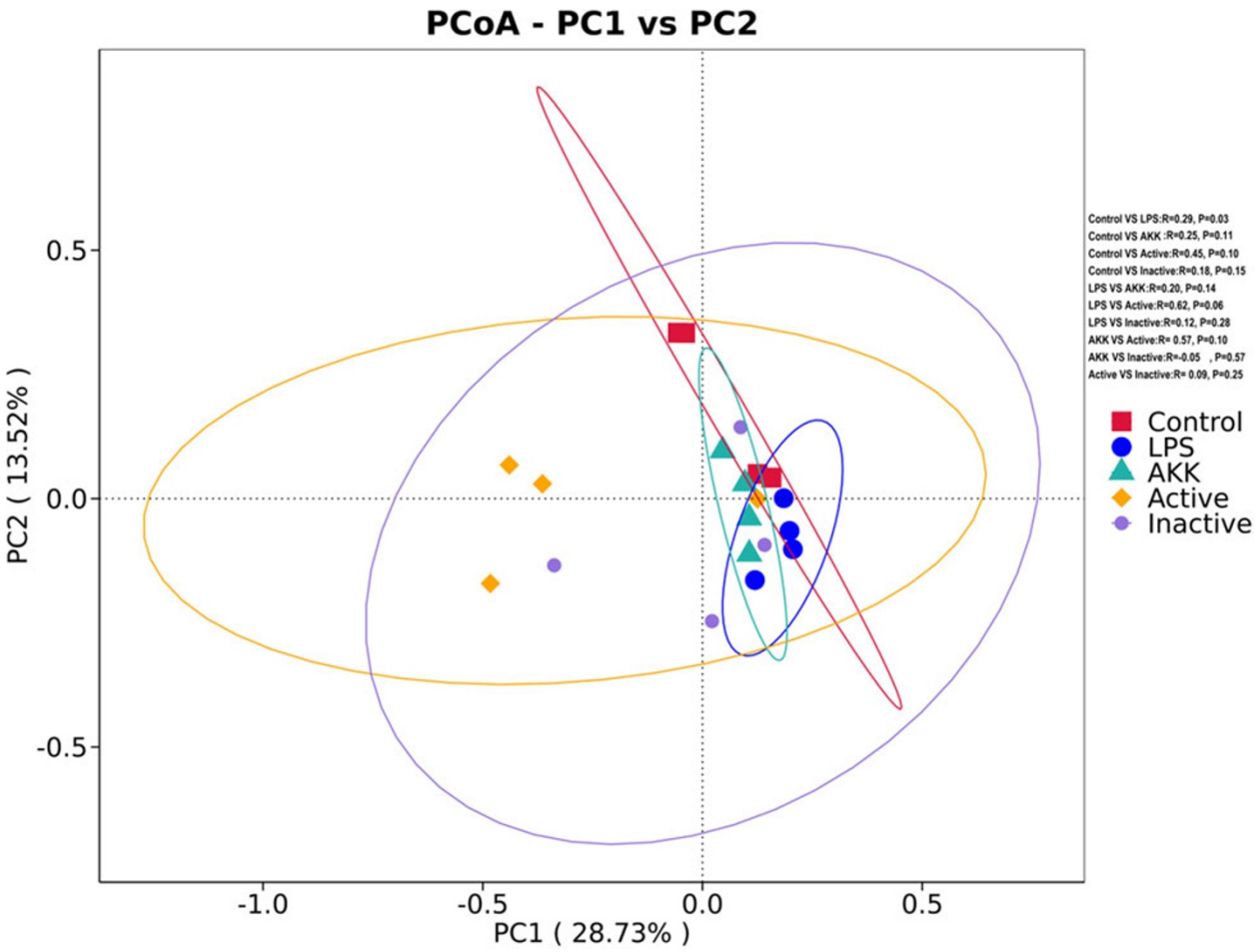


Figure 2. Principal coordinates analysis (PCoA) of the gut microbiota in different groups.

Table 5. Effect of *Akkermansia muciniphila* on the composition of the gut microbiota of lipopolysaccharide-challenged yellow-feathered broilers at phylum level

Items (%)	Control	LPS	AKK	Active	Inactive	SEM	*P*
Firmicutes	77.25[a]	71.11[ab]	57.79[bc]	50.48[c]	57.65[bc]	3.258	0.03
Bacteroidota	21.69	27.42	39.51	38.00	36.36	2.575	0.11
Verrucomicrobiota	0.48	0.09	2.24	10.43	5.49	1.908	0.43
Cyanobacteria	0	0	0	0.69	0.0009	0.1368	0.42
Proteobacteria	0.31	1.19	0.33	0.30	0.25	0.135	0.11
Actinobacteriota	0.27	0.18	0.12	0.08	0.12	0.033	0.42
Desulfobacterota	0.0014	0	0	0	0.12	0.024 10	0.43
Campylobacterota	0	0	0	0.0028	0.008	0.001 50	0.39
Patescibacteria	0	0	0	0	0.0028	0.000 56	0.44
Acidobacteriota	0	0	0.0009	0.0014	0.0005	0.000 34	0.66
Others	0	0.0047	0.0057	0.0065	0.0046	0.001 09	0.39

Note: Control: gavage with phosphate-buffered saline (PBS) and intraperitoneal injection of saline; LPS: gavage with PBS and administered intraperitoneally with lipopolysaccharide (LPS); AKK: gavage with *Akkermansia muciniphila* in culture medium and administered intraperitoneally with LPS; Active: gavage with live *Akkermansia muciniphila* resuspended in PBS and administered intraperitoneally with LPS; Inactive: gavage with inactivated *Akkermansia muciniphila* resuspended in PBS and administered intraperitoneally with LPS; SEM: standard error of mean; [a,b,c] Means in the same row with different superscript letters differ significantly ($P < 0.05$).

group's final weight was comparable to the Control group, the other LPS-challenged groups treated with AKK preparations (Active and Inactive) did not fully recover their growth. This suggests that the full therapeutic benefit requires a synergistic effect between the live AKK bacteria and the metabolites present in its culture medium, rather than being attributable to a single component or the bacteria's known weight-regulating functions alone (Cani and de Vos 2017). In our study, the results of alpha diversity showed that

https://doi.org/10.1017/anr.2025.10019 Published online by Cambridge University Press

Table 6. Effect of *Akkermansia muciniphila* on the composition of the gut microbiota of lipopolysaccharide-challenged yellow-feathered broilers at genus level

Items (%)	Control	LPS	AKK	Active	Inactive	SEM	*P*
Bacteroides	5.34	0.0009	9.33	26.96	12.27	3.273	0.08
Alistipes	16.35^{bc}	27.42^{a}	30.17^{a}	11.04^{c}	24.09^{ab}	2.084	0.005
Akkermansia	0.48	0.09	2.24	10.43	5.49	1.908	0.43
Streptococcus	4.13	4.26	1.08	0.61	0.43	0.924	0.52
Ruminococcus_torques_group	6.90	6.69	5.74	3.77	6.47	0.798	0.77
Butyricicoccus	1.58	3.18	3.01	3.93	2.39	0.604	0.83
Intestinimonas	3.90	6.09	1.75	1.36	0.64	0.721	0.08
Ligilactobacillus	0.50	2.80	0.99	2.71	1.39	0.563	0.65
Unidentified_Oscillospiraceae	2.08	1.04	2.06	3.24	1.67	0.401	0.56
Lactobacillus	0.99	1.33	0.51	0.93	0.32	0.248	0.76
Others	57.76^{a}	47.10^{ab}	43.09^{b}	35.00^{b}	44.84^{ab}	2.446	0.037

Note: Control: gavage with phosphate-buffered saline (PBS) and intraperitoneal injection of saline; LPS: gavage with PBS and administered intraperitoneally with lipopolysaccharide (LPS); AKK: gavage with *Akkermansia muciniphila* in culture medium and administered intraperitoneally with LPS; Active: gavage with live *Akkermansia muciniphila* resuspended in PBS and administered intraperitoneally with LPS; Inactive: gavage with inactivated *Akkermansia muciniphila* resuspended in PBS and administered intraperitoneally with LPS; SEM: standard error of mean; ^{a,b,c} Means in the same row with different superscript letters differ significantly ($P < 0.05$).

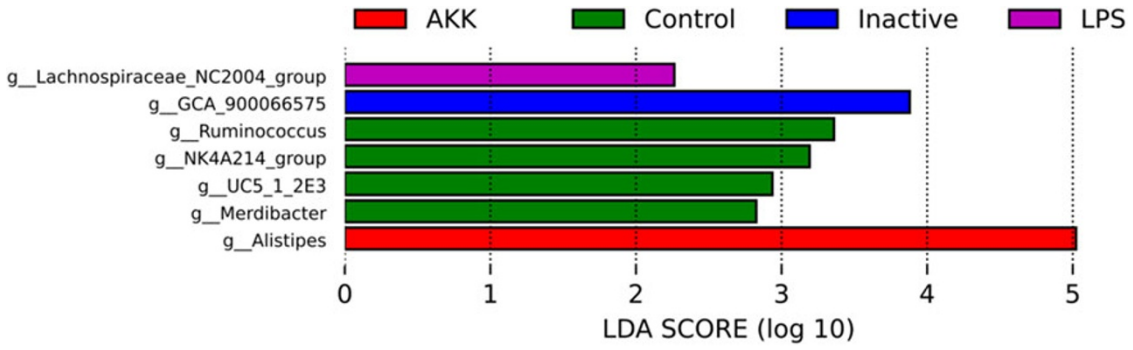


Figure 3. Histogram of linear discriminant analysis distribution of genus level, using default parameters (LDA >2).

the gut microbial composition was similar among the five groups, and there was no significant difference in their richness, diversity and evenness. The abundance of *Firmicutes* was lower in the groups with AKK administration (AKK, Active and Inactive) than in the Control group. While studies have demonstrated increased *Firmicutes* abundance in obese mice (Ley et al. 2005), research indicates that AKK may counteract obesity development (Everard et al. 2013). *Alistipes* suppresses inflammation and ameliorates inflammatory bowel disease, with these effects mediated primarily by the production of SCFAs (Lin et al. 2025). Both genus-level microbial composition analysis and LefSe results revealed significant enrichment of *Alistipes* in the AKK group, whereas its abundance was markedly reduced in the Active group. The AKK intervention may alleviate LPS-induced stress by promoting *Alistipes* proliferation and enhancing the synthesis of SCFAs (e.g., butyrate), thereby suppressing intestinal inflammation through SCFA-mediated mechanisms. Furthermore, microbial composition analysis demonstrated a significant enrichment of *Bacteroides* and a marked reduction in *Streptococcus* abundance in the AKK-gavaged group compared to Controls. *Bacteroides* promotes gut microbial homeostasis (Buzun et al. 2024). Whereas elevated *Streptococcus* abundance is associated with severe atrophic gastritis (Iino et al. 2019). The observed enrichment of *Bacteroides* and depletion of *Streptococcus* in the AKK-gavaged group collectively demonstrate AKK's ability to stabilize gut microbiota.

The intestinal epithelium serves as a dynamic physical and functional barrier, primarily mediated by adherens junctions (e.g., Cadherins) and TJs (e.g., Claudins, Occludin and JAM proteins) (Groschwitz and Hogan 2009). LPS induces intestinal barrier dysfunction by enhancing TJ permeability through a TLR4-dependent signaling pathway, thereby compromising epithelial integrity (Guo et al. 2015). AKK was reported to modulate the intestinal barrier by enhancing the expression of TJ proteins Claudin-3 and Occludin (Chelakkot et al. 2018). In our study, there was no significant difference in the expression of Claudin-1, Claudin-2 and Claudin-3 among the five groups, but the Inactive group had the lowest relative content. Also, the Occludin in the Inactive group was significantly lower than in the other four groups. This indicates that the intestinal barrier function of the jejunum in the Inactive group was weaker than in the other four groups.

KEGG pathway analysis revealed differential regulation of PPAR signaling genes under LPS stimulation, with PLIN1 identified as a significantly upregulated component and APOA1 as a key downregulated factor compared to untreated controls. Studies have shown that APOA1 may exert its anti-inflammatory effects primarily by modulating the function of immune cells (Tao et al. 2024). Its constituent high-density lipoproteins can block the activation of liver inflammation by LPS (Han et al. 2021). PLIN1 may mediate wound inflammatory injury through the NF-κB signaling pathway (Wang et al. 2024). RIG-I-like signaling pathway is

https://doi.org/10.1017/anr.2025.10019 Published online by Cambridge University Press

Table 7. Transcriptome sequencing data quality summary

Sample	raw_reads	raw_bases	clean_reads	clean_bases	Q20 (%)	Q30 (%)	GC_pct (%)
Control1	48,411,234	7.26G	45,796,566	6.87G	99.12	97.5	50.54
Control2	47,116,264	7.07G	45,643,372	6.85G	99.04	97.36	50.64
Control3	43,247,212	6.49G	41,920,242	6.29G	99.11	97.52	50.46
Control4	48,282,708	7.24G	46,051,348	6.91G	99.09	97.46	52.79
LPS1	46,221,914	6.93G	44,783,346	6.72G	99.14	97.59	49.9
LPS2	47,476,674	7.12G	45,562,730	6.83G	99.16	97.63	50.64
LPS3	39,448,692	5.92G	38,225,844	5.73G	99.15	97.63	50.12
LPS4	47,221,778	7.08G	45,671,134	6.85G	99.09	97.48	50.14
AKK1	50,221,598	7.53G	47,471,656	7.12G	99.1	97.49	50.36
AKK2	47,436,454	7.12G	46,365,668	6.95G	99.19	97.69	49.21
AKK3	42,234,912	6.34G	41,034,884	6.16G	99.11	97.51	49.85
AKK4	47,677,650	7.15G	45,984,126	6.9G	99.14	97.57	51.36
Active1	47,096,846	7.06G	45,723,674	6.86G	99.07	97.39	50.15
Active2	48,099,664	7.21G	46,648,836	7.0G	99.15	97.57	50.05
Active3	44,879,824	6.73G	43,181,432	6.48G	99.11	97.51	49.98
Active4	43,142,586	6.47G	42,122,476	6.32G	99.12	97.52	49.95
Inactive1	45,468,360	6.82G	44,110,832	6.62G	99.04	97.33	50.12
Inactive2	46,983,104	7.05G	45,749,692	6.86G	99.06	97.39	49.29
Inactive3	52,469,616	7.87G	50,580,248	7.59G	98.98	97.21	51.21
Inactive4	44,228,924	6.63G	42,241,106	6.34G	99.02	97.32	50.1

Note: raw_reads: number of reads in raw data; raw_bases: number of bases in raw data (raw base = raw reads × 150 bp); clean_reads: number of reads in raw data after filtering; clean_bases: number of bases in raw data after filtering; Q20: percentage of total bases for bases with Phred value greater than 20; Q30: percentage of total bases for bases with Phred value greater than 30; GC_pct: percentage of four bases in clean reads for G and C.

known to enhance antiviral immunity by coordinating type I interferon responses (Kato et al. 2017); its downregulation in the LPS-treated group correlated with exacerbated jejunal inflammation. This suggests that LPS disrupts intestinal immune homeostasis by impairing RIG-I-mediated containment of both viral sensing and inflammatory cascades. Compared to the LPS group, the AKK group demonstrated significant upregulation of two immune-related pathways-the NOD-like receptor signaling pathway and RIG-I-like receptor signaling pathway, with TMEM173 as a shared upregulated gene in both pathways. Transmembrane Protein 173 (TMEM173) plays a critical role in mediating innate immune response to viral and bacterial infections (Okabe et al. 2009). Furthermore, recent studies indicate that the NOD-like receptor signaling pathway is functional in adaptive immune cells and contributes to adaptive immunity (Zhou et al. 2023). Consistent with these findings, our results demonstrated enhanced immune activation in the jejunum of the AKK group compared to the LPS group, as evidenced by the upregulation of TMEM173 and associated pathways. Compared to the LPS group, the Active group exhibited downregulation in drug metabolism, glutathione metabolism and PPAR signaling pathway, while retinol metabolism was significantly upregulated. Drug metabolism involves the biochemical modification of drugs, primarily mediated by cytochrome P450 (Zhao et al. 2021). Glutathione, a pivotal antioxidant maintaining intracellular redox balance, also participates in trained immunity induction through its metabolic regulation (Ferreira et al. 2021). PPAR signaling pathway is a key regulator of anti-inflammatory responses through transcriptional suppression of pro-inflammatory cytokines (Ricote and Glass 2007). These combined results, despite enhanced retinol metabolism, likely contributed to the reduced anti-inflammatory capacity in the Active group. Compared to the LPS group, the ribosome-related pathways and oxidative phosphorylation were significantly enriched and upregulated in the Inactive group. Zhang et al. (2019) reported that genes upregulated in colon adenomas were significantly associated with ribosomal, oxidative phosphorylation-related pathways (Zhang et al. 2019). The coordinated upregulation of these energy-intensive pathways potentially reflects compensatory mechanisms against LPS-induced cellular stress.

GO enrichment analysis revealed a significant upregulation of the defense response to virus pathway in the AKK group compared to the LPS group. Combined with the KEGG results, this indicated that gavage of live AKK bacteria along with their culture medium alleviates LPS-induced intestinal stress by enhancing antiviral defense and modulating innate immune responses. However, the Active group showed downregulation in cellular response to xenobiotic stimulus and oxidoreductase function. Integrating these findings with the observed suppression of PPAR signaling and glutathione metabolism, our data suggested that gavage of live AKK bacteria without culture medium has limited anti-inflammatory capacity, potentially due to compromised detoxification capacity and redox balance. Oxidative phosphorylation, a structural constituent of the ribosome and oxidoreductase activity were upregulated in the Inactive group

https://doi.org/10.1017/anr.2025.10019 Published online by Cambridge University Press

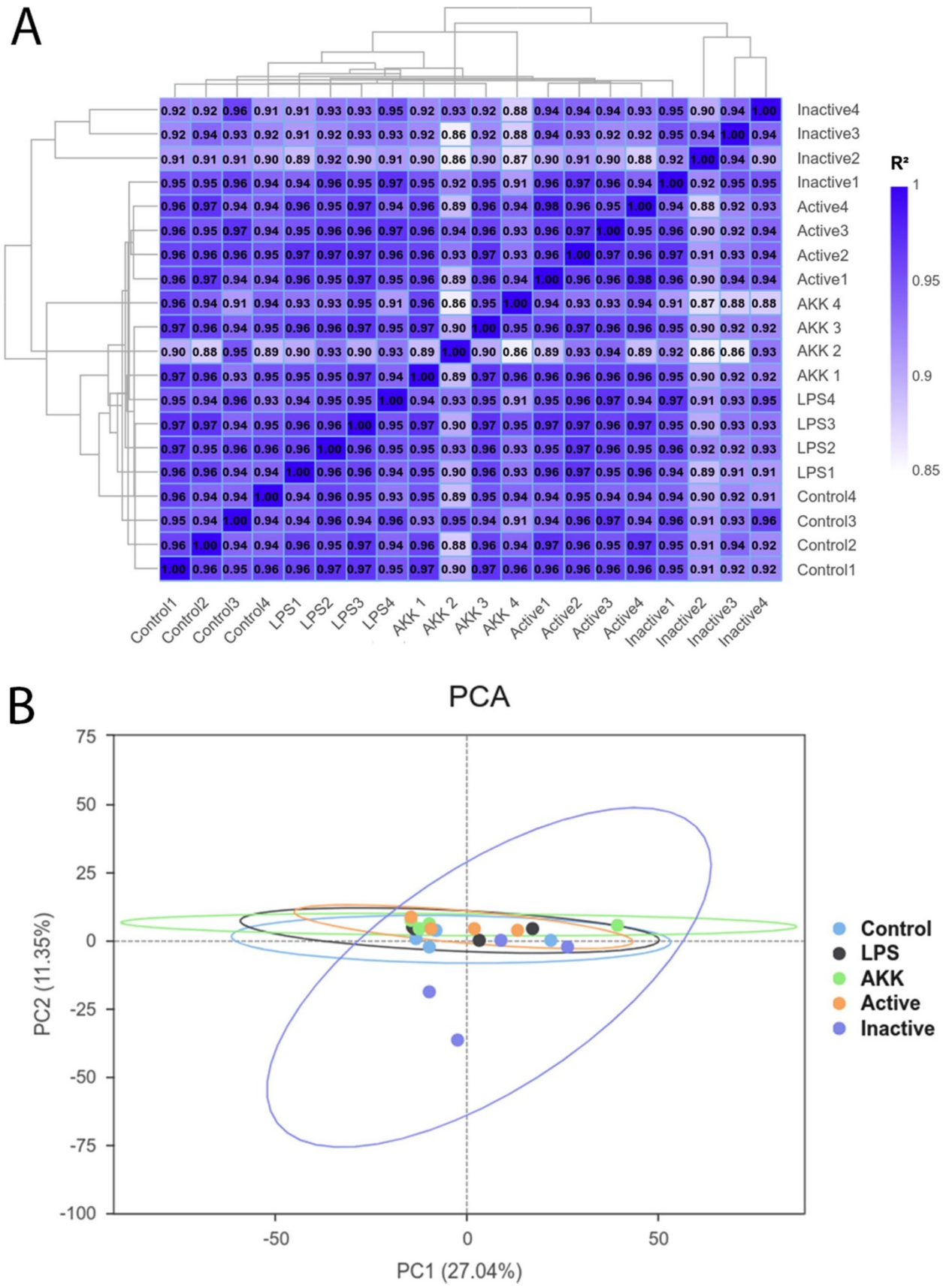


Figure 4. Quantitative analysis of gene expression in different groups. (A) Heat map of correlation between samples. (B) Plot of results of principal component analysis.

https://doi.org/10.1017/anr.2025.10019 Published online by Cambridge University Press

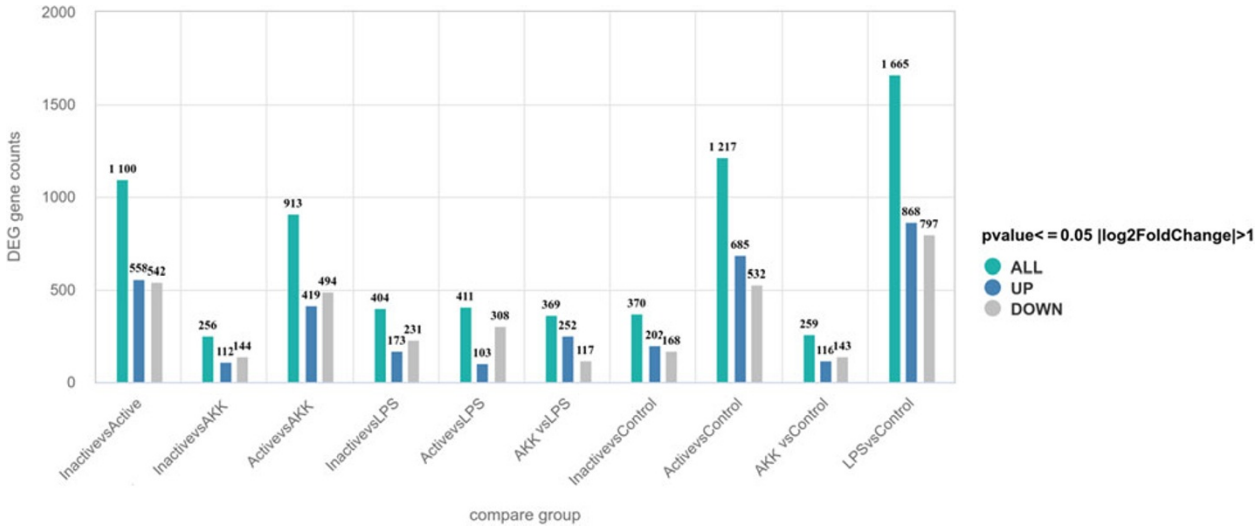


Figure 5. Statistical chart of differentially expressed genes (DEGs) in the differential comparison combinations.

Table 8. Expression of tight junction protein genes in the jejunum

Gene name	Control	LPS	AKK	Active	Inactive	SEM	*P*
Claudin-1	43.50	53.75	45.75	44.75	20.00	4.711	0.21
Claudin-2	1357.00	758.25	1203.75	858.25	925.25	132.683	0.63
Claudin-3	7098.25	5552.25	5008.75	6006.75	4011.25	416.407	0.19
Occludin	5813.25[a]	4500.25[ab]	5540.50[a]	5335.25[a]	3091.75[b]	305.398	0.01

Note: Control: gavage with phosphate-buffered saline (PBS) and intraperitoneal injection of saline; LPS: gavage with PBS and administered intraperitoneally with lipopolysaccharide (LPS); AKK: gavage with *Akkermansia muciniphila* in culture medium and administered intraperitoneally with LPS; Active: gavage with live *Akkermansia muciniphila* resuspended in PBS and administered intraperitoneally with LPS; Inactive: gavage with inactivated *Akkermansia muciniphila* resuspended in PBS and administered intraperitoneally with LPS; SEM: standard error of mean; [a,b] Means within a row with different superscripts are statistically significantly different ($P < 0.05$).

Table 9. Analysis of the top ten Kyoto Encyclopedia of Genes and Genomes (KEGG) enrichment in the four groups

Group	KEGG pathway	−log10 (*P*-value)	Count	Up	Down	Gene
LPS vs Control	Influenza A	2.750	7	0	7	PMLL/SOCS3/PML/RSAD2/EIF2AK2/IFIH1/MX1
	Cysteine and methionine metabolism	2.510	4	3	1	DNMT3B/CDO1/MAT2L/AGXT2
	Taurine and hypotaurine metabolism	1.973	2	2	0	CDO1/GADL1
	PPAR signaling pathway	1.884	4	3	1	APOA1/PLIN1/ME1/APOA2
	Ubiquitin mediated proteolysis	1.871	6	1	5	PMLL/SOCS3/RHOBTB1/PML/UBE2L6/SOCS1
	Herpes simplex virus 1 infection	1.771	6	0	6	PMLL/TMEM173/SOCS3/PML/EIF2AK2/IFIH1
	Pantothenate and CoA biosynthesis	1.604	2	1	1	ENPP1/GADL1
	RIG-I-like receptor signaling pathway	1.444	3	0	3	TMEM173/DHX58/IFIH1
	Sphingolipid metabolism	1.422	3	1	2	LOC121113366/LOC124417438/LOC107049673
	Pyrimidine metabolism	1.320	3	1	2	CMPK2/ENPP1/DCTD
AKK vs LPS	Influenza A	3.421	10	10	0	RSAD2/TLR3/MYD88/EIF2AK2/SOCS3/IFIH1/PMLL/STAT1/MX1/LOC416147
	Pentose and glucuronate interconversions	2.627	4	1	3	LOC107053352/LOC425137/AKR1E2/LOC121111296

(*Continued*)

https://doi.org/10.1017/anr.2025.10019 Published online by Cambridge University Press

Table 9. (*Continued.*)

Group	KEGG pathway	−log10 (*P*-value)	Count	Up	Down	Gene
	Calcium signaling pathway	2.026	9	6	3	CACNA1E/CHRM5/ATP2B4/CACNA1H/PLCD4/P2RX7/FGF1/LOC107053868/FGFR3
	Herpes simplex virus 1 infection	1.866	8	8	0	TMEM173/TLR3/MYD88/EIF2AK2/SOCS3/IFIH1/PMLL/STAT1
	Oxidative phosphorylation	1.852	7	0	7	ATP5I/UQCRHL/ND3/ATP8/CYTB/COX3/ND4L
	Neuroactive ligand-receptor interaction	1.835	9	3	6	GPR25/CHRM5/SST1/GPR83L/GIP/P2RX7/F2RL2/LOC124416959/LOC107053868
	Folate biosynthesis	1.765	3	1	2	LOC107053352/LOC425137/AKR1E2
	NOD-like receptor signaling pathway	1.706	7	7	0	TMEM173/MYD88/GBP4L/LOC121106625/STAT1/P2RX7/LOC121106623
	Cytosolic DNA-sensing pathway	1.645	4	4	0	DNASE2B/TMEM173/SAMHD1/CCL4
	RIG-I-like receptor signaling pathway	1.588	4	4	0	TMEM173/DHX58/IFIH1/LOC416147
Active vs LPS	Glutathione metabolism	3.849	5	1	4	GSTA3/GSTA4/CHAC1/GSTA2/HPGDS
	Drug metabolism – cytochrome P450	3.416	4	0	4	GSTA3/GSTA4/GSTA2/HPGDS
	Drug metabolism – other enzymes	3.321	5	0	5	GSTA3/GSTA4/GSTA2/DPYS/UPP2
	Metabolism of xenobiotics by cytochrome P450	3.268	4	0	4	GSTA3/GSTA4/GSTA2/HPGDS
	PPAR signaling pathway	2.381	4	0	4	LOC121108229/PLIN1/ACSL6/APOA2
	Glycine, serine and threonine metabolism	2.258	3	0	3	GLDC/AGXT2/CYLY
	Retinol metabolism	2.154	3	3	0	RP11-400G3.5/LOC121113132/RPE65
	Cysteine and methionine metabolism	1.945	3	0	3	AGXT2/MAT1A/CYLY
	Ferroptosis	1.365	2	0	2	NCOA4/ACSL6
Inactive vs LPS	Ribosome	14.321	35	35	0	RPL14/RPS7/RPS24/RPS8/RPL9/RPL19/RPL35A/RPL31/RPL37/RPS15/RPS27/RPS28/RPS27A/RPS25/RPL21/RPS15A/RPL13/RPL23/RPS17/RPL26L1/RPS10/RPL22/RPL29/RPL8/RPL37A/RPL27/RPL17/RPLP1/RPL36/RPL32/RPS11/RPL38/MRPS12/MRPL24/MRPL2
	Oxidative phosphorylation	4.834	21	20	1	ND6/ND1/COX1/COX3/ND5/ATP6/CYTB/COX2/ND4/ND3/ND2/NDUFA7/ATP8/ND4L/NDUFS5/UQCR10/ATP5E/NDUFA1/COX8A/LOC107054664/LOC121109310
	ABC transporters	4.526	11	2	9	ABCA3/ABCC2/ABCG5/ABCA1/ABCD2/ABCB1/ABCC5/ABCG8/ABCB8/ABCB11/LOC121111322
	Cardiac muscle contraction	2.856	10	9	1	COX1/COX3/CYTB/COX2/UQCR10/COX8A/TPM2/ATP2A3/LOC107054664/TNNC1
	Protein processing in endoplasmic reticulum	2.802	20	2	18	CANX/MAN1A2/HSPA5/SAR1B/SEL1L/WFS1/PDIA6/YOD1/ERLEC1/MAN1A1/RPN2/LMAN1L/BAG2/P4HB/SEC61G/EIF2AK3/DDOST/LOC121106746/MAGT1/LOC121107129
	ECM-receptor interaction	2.651	12	0	12	CD47/ITGB6/ITGB4/ITGA6/LAMC2/ITGAV/CHAD/LAMB3/CD36/ITGA4/THBS2/LOC121113411
	Various types of N-glycan biosynthesis	1.881	7	0	7	MAN1A2/MAN2A1/MAN1A1/RPN2/DDOST/HEXA/MAGT1
	Cell adhesion molecules	1.838	13	3	10	GLG1/ITGA6/ITGAV/BLB1/CDH1/CLDN1/ALCAM/CD6/ITGA4/NLGN3/CLDN12/LOC121113411/CLDN5

(*Continued*)

https://doi.org/10.1017/anr.2025.10019 Published online by Cambridge University Press

Table 9. (*Continued.*)

Group	KEGG pathway	−log10 (*P*-value)	Count	Up	Down	Gene
	Sphingolipid metabolism	1.740	8	0	8	LOC121113366/PSAP/SPTLC2/GLB1/GALC/ASAH1/ HEXA/LOC121108934
	Ascorbate and aldarate metabolism	1.639	4	1	3	LOC101749599/RGN/LOC121111295/UGT1A1

Note: Control: gavage with phosphate-buffered saline (PBS) and intraperitoneal injection of saline; LPS: gavage with PBS and administered intraperitoneally with lipopolysaccharide (LPS); AKK: gavage with *Akkermansia muciniphila* in culture medium and administered intraperitoneally with LPS; Active: gavage with live *Akkermansia muciniphila* resuspended in PBS and administered intraperitoneally with LPS; Inactive: gavage with inactivated *Akkermansia muciniphila* resuspended in PBS and administered intraperitoneally with LPS; SEM: standard error of mean.

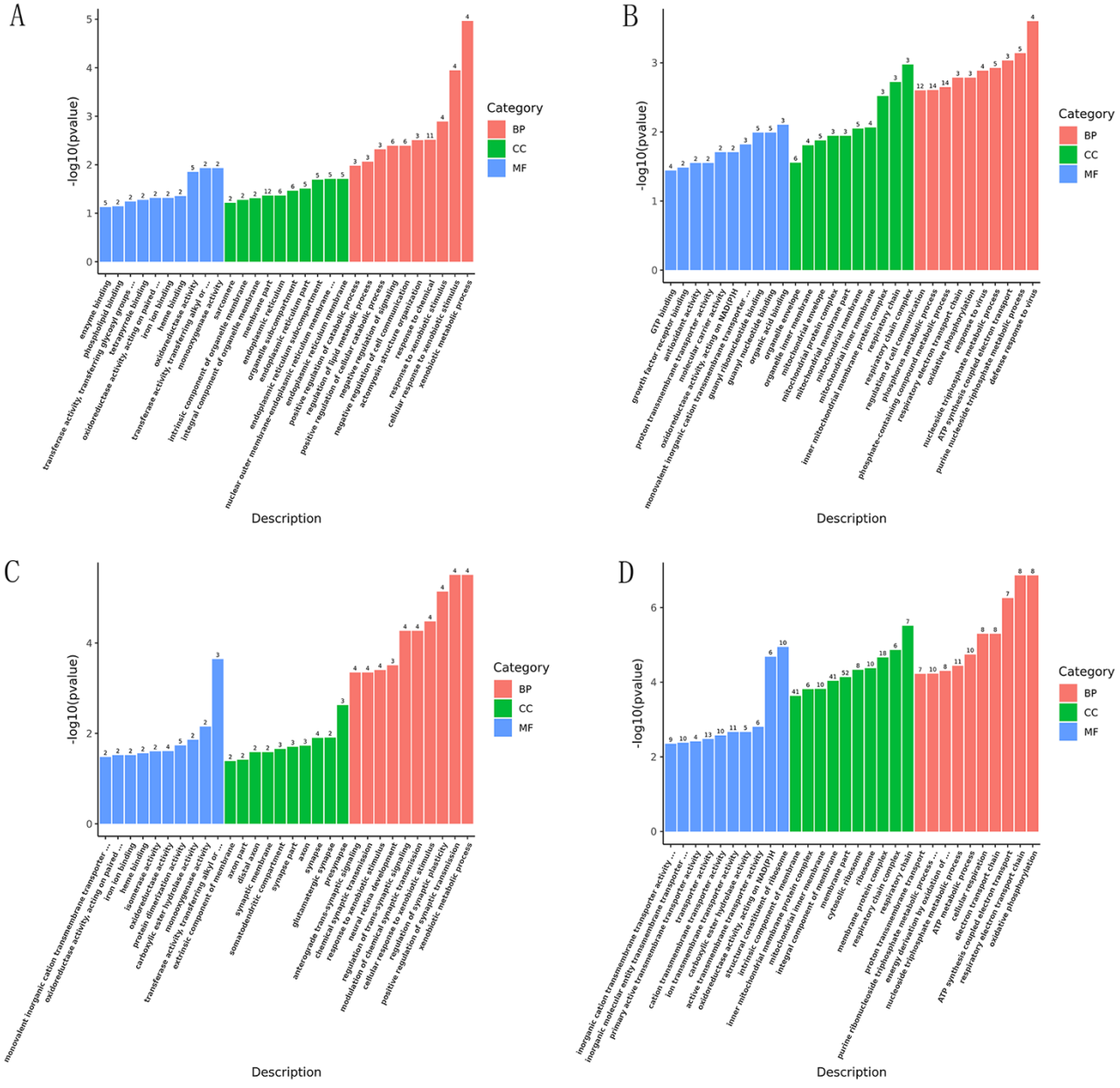


Figure 6. Gene Ontology (GO) enrichment analysis of differentially expressed genes (DEGs). The four comparison groups are: (A) LPS vs Control; (B) AKK vs LPS; (C) Active vs LPS; and (D) Inactive vs LPS. The analysis covers three categories: biological process (BP), cellular component (CC), and molecular function (MF).

compared to the LPS group. Mitochondrial ribosomes are essential for translating oxidative phosphorylation components, while tumor cells exhibit hyperactive ribosome biogenesis to meet their biosynthetic demands (Pecoraro et al. 2021). Combined with prior findings, these data suggested that the Inactive group exhibited compromised resistance to LPS-induced inflammation

https://doi.org/10.1017/anr.2025.10019 Published online by Cambridge University Press

and displayed metabolic signatures suggestive of oncogenic predisposition.

While studies report that AKK reduces LPS-induced intestinal stress (Hu et al. 2025), our findings revealed that AKK, with its culture medium, enhanced intestinal immunity more effectively than AKK alone. This disparity may be related to bioactive components in the culture medium, such as SCFAs and extracellular vesicles. It has been shown that AKK produces SCFAs by degrading mucins (Zhang et al. 2019), and SCFAs play a role in intestinal immunity and anti-inflammation (Sam et al. 2021). Both SCFAs and extracellular vesicles can improve gut barrier function via Occludin-AMPK signaling (Chelakkot et al. 2018; Voltolini et al. 2012). Further studies are needed to clarify the exact mechanisms.

Nevertheless, some limitations of this study should be considered. Our investigation utilized a single strain of AKK (ATCC BAA-835), and the observed benefits may not be entirely generalizable, as the functional properties of probiotics can be highly strain-specific. Future comparative studies using multiple strains would be valuable. Additionally, the acute LPS challenge model, while effective for inducing an inflammatory response, represents a simplified simulation of the complex, multifactorial gut health challenges found in commercial poultry production. Therefore, the protective effects of AKK warrant further validation in more diverse and commercially relevant stress or disease models. These limitations provide a clear direction for future research to build upon our foundational findings.

Conclusions

In this study, we investigated the effects of different preparations of AKK on LPS-induced intestinal stress in broilers through gut microbiome and jejunal transcriptome analysis. All three groups stabilized gut microbiota in broilers under LPS challenge, especially the AKK with its culture medium group. Oral administration of live AKK with its culture medium effectively alleviated LPS-induced jejunal stress by enhancing antiviral defense pathways, whereas live AKK without culture medium exhibited weaker anti-inflammatory effects. In contrast, heat-inactivated AKK without medium failed to mitigate jejunal stress, underscoring the importance of bacterial viability and culture medium components for therapeutic efficacy.

Data Availability Statement. The data that support the findings of this study (Reference No. PRJNA1194789, PRJNA1202580) can be found at http://www.ncbi.nlm.nih.gov/bioproject/1194789, http://www.ncbi.nlm.nih.gov/bioproject/1202580.

Author Contributions. R.Z. drafted the manuscript. J.T., Y.J. and L.O. conducted the study and collected samples. C.L. and Z.Z. analyzed the samples and performed data analysis. X.F. reviewed and revised the manuscript. All authors read and approved the final manuscript.

Competing Financial Interests. The authors declare no competing financial interests.

Ethical Standards. This experimental protocol was approved by the Ethical Committee and conducted under the supervision of the Institutional Animal Care and Use Committee of Foshan University (#FOSU202421002, Foshan, China).

References

Aggarwal V, Sunder S and Verma SR (2022) Disease-associated dysbiosis and potential therapeutic role of Akkermansia muciniphila, a mucus degrading bacteria of gut microbiome. *Folia Microbiol (Praha)* **67**, 811–824.

Buzun E, Hsu CY, Sejane K *et al.* (2024) A bacterial sialidase mediates early-life colonization by a pioneering gut commensal. *Cell Host & Microbe* **32**. https://doi.org/10.1016/j.chom.2023.12.014

Cani PD and de Vos WM (2017) Next-generation beneficial microbes: the case of Akkermansia muciniphila. *Frontiers in Microbiology* **8**, https://doi.org/10.3389/fmicb.2017.01765

Chelakkot C, Choi Y, Kim DK *et al.* (2018) Akkermansia muciniphila-derived extracellular vesicles influence gut permeability through the regulation of tight junctions. *Experimental and Molecular Medicine* **50**, e450.

Douglas GM, Maffei VJ, Zaneveld JR *et al.* (2020) PICRUSt2 for prediction of metagenome functions. *Nature Biotechnology* **38**, 685–688.

Elokil A, Li SJ, Chen W *et al.* (2024) Ethoxyquin attenuates enteric oxidative stress and inflammation by promoting cytokine expressions and symbiotic microbiota in heat-stressed broilers. *Poultry Science* **103**. https://doi.org/10.1016/j.psj.2024.103761

Everard A, Belzer C, Geurts L *et al.* (2013) Cross-talk between and intestinal epithelium controls diet-induced obesity. *Proceedings of the National Academy of Sciences of the United States of America* 110, 9066–9071.

Ferreira AV, Koeken VACM, Matzaraki V *et al.* (2021) Glutathione metabolism contributes to the induction of trained immunity. *Cells* **10**. https://doi.org/10.3390/cells10050971

Gabriel I, Lessire M, Mallet S *et al.* (2006) Microflora of the digestive tract: Critical factors and consequences for poultry. *Worlds Poultry Science Journal* **62**, 499–511.

Groschwitz KR and Hogan SP (2009) Intestinal barrier function: Molecular regulation and disease pathogenesis. *Journal of Allergy and Clinical Immunology* **124**, 3–20.

Guo SH, Nighot M, Al-Sadi R *et al.* (2015) Lipopolysaccharide regulation of intestinal tight junction permeability is mediated by TLR4 signal transduction pathway activation of FAK and MyD88. *Journal of Immunology* **195**, 4999–5010.

Han YH, Onufer EJ, Huang LH *et al.* (2021) Enterically derived high-density lipoprotein restrains liver injury through the portal vein. *Science* **373**, 410–+.

Hu Y, Zhou J and Lin X (2025) *Akkermansia muciniphila* helps in the recovery of lipopolysaccharide-fed mice with mild intestinal dysfunction. *Frontiers in Microbiology* **16**: 1523742.

Iino C, Shimoyama T, Chinda D *et al.* (2019) Influence of *helicobacter pylori* Infection and atrophic gastritis on the gut microbiota in a Japanese population. *Helicobacter* **101**(4), 422–432.

Kato H, Oh SW and Fujita T (2017) RIG-I-Like receptors and type I interferonopathies. *Journal of Interferon & Cytokine Research* **37**, 207–213.

Kikusato M and Toyomizu M (2023) Mechanisms underlying the effects of heat stress on intestinal integrity, inflammation, and microbiota in chickens. *Journal of Poultry Science* **60**. https://doi.org/10.2141/jpsa.2023021

Ley RE, Bäckhed F, Turnbaugh P *et al.* (2005) Obesity alters gut microbial ecology. *Proceedings of the National Academy of Sciences of the United States of America* 102:11070–11075.

Li MJ, Shao DT, Zhou JC *et al.* (2020) Signatures within esophageal microbiota with progression of esophageal squamous cell carcinoma. *Chinese Journal of Cancer Research* **32**, 755–767.

Lin XY, Xu MC, Lan RT *et al.* (2025) Gut commensal improves experimental colitis in mice with reduced intestinal epithelial damage and cytokine secretion. *Msystems*. https://doi.org/10.1128/msystems.01607-24

Lukovac S, Belzer C, Pellis L *et al.* (2014) Differential Modulation by Akkermansia muciniphila and faecalibacterium prausnitzii of host peripheral lipid metabolism and histone acetylation in mouse gut organoids. *mBio* **5**. https://doi.org/10.1128/mBio.01438-14

Ma QM, Zhou XC, Su WK *et al.* (2025) Akkermansia muciniphila inhibits jejunal lipid absorption and regulates jejunal core bacteria. *Microbiological Research* **293**. https://doi.org/10.1016/j.micres.2025.128053

Mishra B and Jha R (2019) Oxidative stress in the poultry gut: Potential challenges and interventions. *Frontiers in Veterinary Science* **6**. https://doi.org/10.3389/fvets.2019.00060

https://doi.org/10.1017/anr.2025.10019 Published online by Cambridge University Press

Okabe Y, Sano T and Nagata S (2009) Regulation of the innate immune response by threonine-phosphatase of eyes absent. *Nature* **460**, 520–U599.

Ottman N, Reunanen J, Meijerink M *et al.* (2017) Pili-like proteins of modulate host immune responses and gut barrier function. *Plos One* **12**. https://doi.org/10.1371/journal.pone.0173004

Parkhomchuk D, Borodina T, Amstislavskiy V *et al.* (2009) Transcriptome analysis by strand-specific sequencing of complementary DNA. *Nucleic Acids Research* **37**. https://doi.org/10.1093/nar/gkp596

Pecoraro A, Pagano M, Russo G *et al.* (2021) Ribosome biogenesis and cancer: Overview on ribosomal proteins. *International Journal of Molecular Sciences* **22**. https://doi.org/10.3390/ijms22115496

Plovier H, Everard A, Druart C *et al.* (2017) A purified membrane protein from or the pasteurized bacterium improves metabolism in obese and diabetic mice. *Nature Medicine* **23**, 107–113.

Ricote M and Glass CK (2007) PPARs and molecular mechanisms of transrepression. *Biochimica Et Biophysica Acta-Molecular and Cell Biology of Lipids* **1771**, 926–935.

Sam QH, Ling H, Yew WS *et al.* (2021) The divergent immunomodulatory effects of short chain fatty acids and medium chain fatty acids. *International Journal of Molecular Sciences* **22**. https://doi.org/10.3390/ijms22126453

Segata N, Izard J, Waldron L *et al.* (2011) Metagenomic biomarker discovery and explanation. *Genome Biology* **12**. https://doi.org/10.1186/gb-2011-12-6-r60

Shen J, Tong XD, Sud N *et al.* (2016) Low-density lipoprotein receptor signaling mediates the triglyceride-lowering action of in genetic-induced hyperlipidemia. *Arteriosclerosis Thrombosis and Vascular Biology* **36**, 1448–+.

Song W, Chen J, Ai G *et al.* (2025) Mechanisms of the effects of turpiniae folium extract on growth performance, immunity, antioxidant activity and intestinal barrier function in LPS-challenged broilers. *Poultry Science* **104**, 104903.

Tao X, Tao R, Wang KY *et al.* (2024) Anti-inflammatory mechanism of Apolipoprotein A-I. *Frontiers in Immunology* **15**. https://doi.org/10.3389/fimmu.2024.1417270

Trojánek Z, Kovaríik A, Spanová A *et al.* (2018) Application of magnetic polymethacrylate-based microspheres for the isolation of DNA from raw vegetables and processed foods of plant origin. *Journal of Food Processing and Preservation* **42**. https://doi.org/10.1111/jfpp.13384

Voltolini C, Battersby S, Etherington SL *et al.* (2012) A novel antiinflammatory role for the short-chain fatty acids in human labor. *Endocrinology* **153**, 395–403.

Wang MT, Cao XL, Shang YX *et al.* (2024) Correlational analysis of PLIN1 with inflammation in diabetic foot ulcer wounds. *Diabetes Research and Clinical Practice* **209**. https://doi.org/10.1016/j.diabres.2024.111605

Zhang FH and Wang DL (2023) Potential of and its outer membrane proteins as therapeutic targets for neuropsychological diseases. *Frontiers in Microbiology* **14**: 1191445.

Zhang L, Li QQ, Cheng L *et al*. (2019) *Akkermansia muciniphila* is a promising probiotic *Microbial Biotechnology* **12**, 1109–1125.

Zhang L-Z, Gong J-G, Li J-H *et al.* (2023) Dietary resveratrol supplementation on growth performance, immune function and intestinal barrier function in broilers challenged with lipopolysaccharide. *Poultry Science* **102**, 102968.

Zhang YD, Wu WX and Qu H (2019) Integrated analysis of the gene expression changes during colorectal cancer progression by bioinformatic methods. *Journal of Computational Biology* **26**, 1168–1176.

Zhao MZ, Ma JS, Li M *et al.* (2021) Cytochrome P450 enzymes and drug metabolism in humans. *International Journal of Molecular Sciences* **22**. https://doi.org/10.3390/ijms222312808

Zhou YJ, Yu SY and Zhang WY (2023) NOD-like receptor signaling pathway in gastrointestinal inflammatory diseases and cancers. *International Journal of Molecular Sciences* **24** (19), 14511.

https://doi.org/10.1017/anr.2025.10019 Published online by Cambridge University Press